Pharmaceutical Research, Vol. 27, No. 4, April 2010 (© 2009)
DOI: 10.1007/s11095-009-0021-1

Research Paper

Understanding the Behavior of Amorphous Pharmaceutical Systems during Dissolution

David E. Alonzo,[1] Geoff G. Z. Zhang,[2] Deliang Zhou,[3] Yi Gao,[2,4] and Lynne S. Taylor[1,4]

Received August 31, 2009; accepted November 30, 2009; published online February 12, 2010

Purpose. To investigate the underlying physical processes taking place during dissolution of amorphous pharmaceuticals and correlate them to the observed solution concentration-time profiles. Felodipine and indomethacin were used as model hydrophobic compounds.
Methods. Concentration-time profiles were monitored during dissolution of the model amorphous compounds using *in situ* fiber-optic ultraviolet spectroscopy. Crystallization of the solid exposed to an aqueous environment was monitored using Raman spectroscopy and/or powder X-ray diffraction. Polarized light microscopy was used to provide qualitative information about crystallization processes.
Results. For felodipine, a small extent of supersaturation was generated via dissolution at 25°C but not at 37°C. The amorphous solid was found to crystallize rapidly at both temperatures upon exposure to the dissolution medium. Addition of low concentrations of polymers to the dissolution medium was found to delay crystallization of the amorphous solid, leading to the generation of supersaturated solutions. Amorphous indomethacin did not crystallize as readily in an aqueous environment; hence, dissolution resulted in supersaturated solutions. However, crystallization from these supersaturated solutions was rapid. Polymeric additives were able to retard crystallization from supersaturated solutions of both indomethacin and felodipine for up to 4 h.
Conclusions. The dissolution advantage of amorphous solids can be negated either by crystallization of the amorphous solid on contact with the dissolution medium or through rapid crystallization of the supersaturated solution. Polymeric additives can potentially retard both of these crystallization routes, leading to the generation of supersaturated solutions that can persist for biologically relevant timeframes.

KEY WORDS: amorphous; dissolution; felodipine; indomethacin; metastable; polymer; supersaturation.

INTRODUCTION

Strategies for increasing the bioavailability of pharmaceutical compounds by solubility/dissolution enhancement are extremely important to the pharmaceutical industry. Many active pharmaceutical ingredients (APIs) with important therapeutic targets are poorly soluble, and a method for overcoming this issue would make these APIs more viable candidates for development (1,2). Amorphous materials are attractive for solubility enhancement since they can generate solution concentrations many times greater than their crystalline counterparts (3–5). This increased effective solubility has been shown in several *in vivo* studies to have a direct impact on bioavailability (5–9). However, a number of challenges need to be addressed in order to take advantage of amorphous materials. For example, one major issue associated with amorphous APIs is that they are inherently metastable, which can lead to phase transformations during storage as well as during dissolution. Although there has been a significant amount of research conducted on the physical stability of amorphous pharmaceuticals under storage conditions (10–14), much less attention has been given to the *in vitro* and *in vivo* behavior of these amorphous materials during dissolution. As a result, there is an insufficient understanding of the processes governing the resultant concentration-time profiles.

Although it has been demonstrated that amorphous pharmaceuticals can provide faster dissolution rates and higher solution concentrations than their crystalline counterparts, as mentioned earlier, there are several potential issues (15). First, when introduced to aqueous media, amorphous APIs have a tendency to crystallize via a solid-to-solid transition. If this phase transition takes place rapidly, the observed supersaturation will be much lower than that expected based on theoretical estimates. If the crystallization rate of the solid is extremely rapid, it is possible that no supersaturation will be observed. Although extremely important, detailed investigation and analysis into the phase

Electronic supplementary material The online version of this article (doi:10.1007/s11095-009-0021-1) contains supplementary material, which is available to authorized users.

[1] Department of Industrial and Physical Pharmacy, School of Pharmacy, Purdue University, 575 Stadium Mall Drive, West Lafayette, Indiana 47907, USA.
[2] Global Pharmaceutical R&D, Abbott Laboratories, 100 Abbott Park Road, Abbott Park, Illinois 60064, USA.
[3] Global Pharmaceutical Operation, Abbott Laboratories, 100 Park Road, Abbott, Illinois 60064, USA.
[4] To whom correspondence should be addressed. (e-mail: gao.yi@abbott.com; lstaylor@purdue.edu)

behavior of pharmaceutical solids during dissolution is very limited (16–19). In order to prevent crystallization of the amorphous phase, polymers are usually incorporated into the matrix as stabilizers (20–23). These polymers are usually designed to provide stabilization of the amorphous drug during storage. However, stabilization of the solid phase during dissolution is equally as important and should be as much of a consideration for formulators as stabilization during storage. Therefore, elucidating how the polymer interacts with amorphous solids in an aqueous medium is of interest from this perspective. A second potential issue with amorphous formulations is that once supersaturation is generated, there will be a thermodynamic driving force for crystallization from solution to a more stable crystalline form. If elevated solution concentrations are not maintained for a sufficient period of time to provide an increase in bioavailability, then the benefits of using high energy amorphous materials as "solubility enhancers" will be marginal at best.

The purpose of this research was to gain an understanding of the phase behavior of amorphous solids during dissolution and how this behavior impacts the resultant solution concentration-time profiles. It is hypothesized that the level of supersaturation attained during dissolution of an amorphous solid depends on the crystallization rate of the solid as well as the tendency of the supersaturated solution to crystallize. Furthermore, the observed concentration-time profiles will be determined by the rates of the phase transformations mentioned above relative to the rate of dissolution. Felodipine and indomethacin were selected as the model compounds because of their low aqueous solubility. Dissolution profiles of these two APIs were evaluated in the presence and absence of polymeric additives at 25°C and 37°C.

MATERIALS AND METHODS

Felodipine was a provided by AstraZeneca, Södertälje, Sweden. Indomethacin was purchased from Hawkins Pharmaceutical (Hawkins Inc., Minneapolis, MN). Polyvinylpyrrolidone (PVP) K29/32 was purchased from Sigma Aldrich Co. (St. Louis MO, USA), while hydroxypropylmethyl cellulose (HPMC) Pharmacoat grade 606 and hydroxypropylmethyl cellulose acetate succinate (HPMC-AS) MF grade were supplied by Shin Etsu (Shin-Etsu Chemical Co., Ltd., Tokyo, Japan). The dissolution medium (with and without pre-dissolved polymer) used in all of the following experiments was 20 mL of 50 mM pH 6.8 phosphate buffer for felodipine and 50 mL of 50 mM pH 2 phosphate buffer for indomethacin. In the case of felodipine, polymer concentrations were either 500 μg/mL (0.05% w/v) or 1,000 μg/mL (0.1% w/v). In the case of indomethacin, polymer concentrations were 250 μg/mL (0.025% w/v). Molecular structures of the model compounds and polymers are shown in Fig. 1.

Preparation of Amorphous Solids

Samples of amorphous felodipine and indomethacin were prepared by heating the crystalline API to 10°C above the melting temperature followed by quench cooling. Samples were cryo-milled with a Spex model 6750 cryo-mill for 30 s at 3 impacts per second for 3 cycles (SPEX CertiPrep LLC, Metuchen, NJ) and then sieved; the particle size range 100–300 μm was retained. The amorphous material was then stored in desiccators containing Drie-Rite® in a refrigerator or freezer until analyzed. The amorphous nature of the materials was verified using powder X-ray diffraction or cross-polarized light microscopy prior to use.

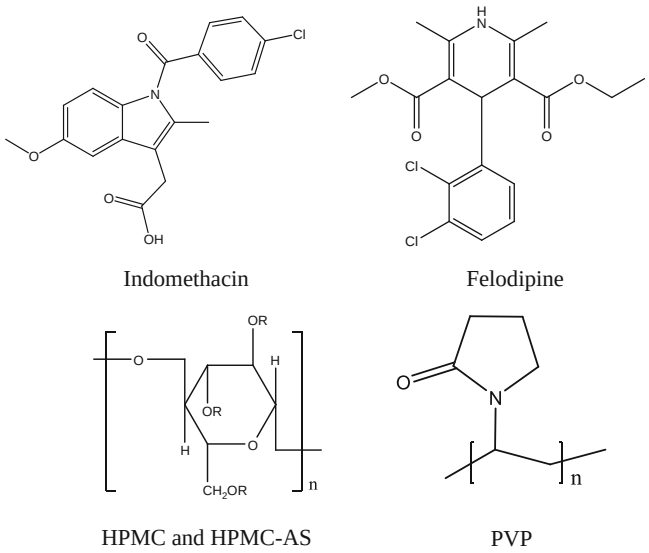

Fig. 1. Molecular structures of indomethacin, felodipine, PVP, HPMC and HPMC-AS. Polymer molecular weights and substitution information were compiled by Konno *et al.* (20).

Powder X-Ray Diffraction (PXRD)

PXRD data were collected using a G3000 diffractometer (Inel Corp., Artenay, France) equipped with a curved position-sensitive detector and parallel beam optics. The diffractometer was operated with a copper anode tube (1.5 kW fine focus) at 40 kV and 30 mA. An incident beam germanium monochrometer provided monochromatic radiation. The diffractometer was calibrated using the attenuated direct beam at one-degree intervals. Calibration was checked using a silicon powder line position reference standard (NIST 640c). The instrument was computer-controlled using the Symphonix software (Inel Corp., Artenay, France), and the data was analyzed using the Jade software (version 6.5, Materials Data, Inc., Livermore, CA). A sample of amorphous felodipine was loaded onto an aluminum sample holder and leveled with a glass slide. The amorphous material was then exposed to the dissolution media by adding 3–4 drops of solution in the presence and absence of 1 mg/mL HPMC-AS or PVP. Data collection began 15 min after the initial exposure.

Raman Spectroscopy

Phase transformations of slurried amorphous felodipine and indomethacin were monitored using a RamanRxn-785 Raman Spectrometer (Kaiser Optical Systems, Inc., Ann Arbor, MI) with a laser wavelength of 785 nm. Slurries consisted of approximately 500 mg to 750 mg of solid and 2 mL or 5 mL of solution for felodipine and indomethacin, respectively. The spectra were collected using a fiber-optic MR probe coupled with a sapphire-tipped immersion probe. Holograms software (Version 4.0, Kaiser Optical Systems,

Inc., Ann Arbor, MI) was used to control the Raman spectrometer. The probe was immersed in a slurry of amorphous material that was exposed to the dissolution medium in the presence and absence of the aforementioned polymers at both 25°C and 37°C. Spectra were collected every minute until the transformation was complete or 4 h had gone by. In the case of felodipine, a partial-least-squares (PLS) calibration was built with SIMCA P + V. 12 software (Umetrics Inc., Umea Sweden). Mixtures of amorphous and crystalline felodipine composed of 0%, 10%, 25%, 50%, 75%, 90% and 100% crystalline felodipine were used as calibration standards. Three independent sets of these standards were prepared by cryo-milling the mixtures. A standard normal variate correction was performed on the mean centered data in order to minimize fluctuations in spectral intensity. For the model, one principal component was found to describe 96.4% of the variation in the data R2Y(cum), with a Q2(cum) (fraction of the total variation in the y variable that can be predicted by the model) of 0.959 and a root mean square error of the estimation (RMSEE) of 7.21. Indomethacin spectra had fluorescent backgrounds, making PLS modeling difficult. In order to obtain a qualitative profile of the transformation kinetics in this system, a univariate approach was used. First, the data was unit-normalized, followed by a baseline correction whereby the intensity values at 1,730 cm^{-1} were subtracted from a peak at 1,648 cm^{-1} that is characteristic of the alpha form of indomethacin. This corrected peak intensity for the alpha form was then plotted *vs.* time.

Microscopy

A Nikon Eclipse E600 Pol microscope with 10x magnification was used with NIS-Elements version 2.3 software package (Nikon Co., Tokyo, Japan). Amorphous indomethacin samples were analyzed using polarized light with an analyzer set to 90° with respect to the polarizer and a λ (530 nm) tint plate at room temperature. The amorphous material was placed on a microscope slide and then exposed to phosphate buffer in the presence or absence of the polymers mentioned above. Images were taken at various time intervals in order to observe the transformation behavior. AVI videos from an experiment in the absence of polymer were taken and are available online in Supplementary Material. Select images from this video were extracted and included in the results section.

UV Spectroscopy

Dissolution experiments for amorphous felodipine were carried out using a pION μ-Diss Profiler (pION Inc.,Woburn, MA) equipped with a 6-channel fiber-optic probe system, heating blocks and magnetic stirrers (500 rpm). For amorphous indomethacin, dissolution experiments were conducted in a jacketed flask (connected to a circulating water bath), and a Corning stir plate was used for stirring. Concentration monitoring was achieved via a SI-Photonics UV spectrometer equipped with a single fiber-optic probe (SI Photonics INC, Tuscon, AZ). In addition, the effect of polymers on crystallization from solution was evaluated for indomethacin by generating a supersaturated solution through addition of a small volume of indomethacin dissolved in MeOH (less than 1 ml) to a buffered solution at pH 2 containing the polymer at a concentration of 250 μg/mL. The concentration-time profiles were monitored using the aforementioned SI Photonics system. Wavelength scans were performed at 1 min time intervals for all experiments (for clarity, not all of these data points are included in the graphs presented in the results section). Second derivatives of the spectra were taken for the calibration as well as the sample data in order to mitigate particle scattering effects. Calibration solutions were prepared in methanol for both APIs investigated. Dissolution media were equilibrated at 37°C or 25°C prior to addition of the API. API (either in the amorphous form or pre-dissolved in methanol) was then added to the dissolution media, and data collection commenced immediately.

Estimation of Amorphous Solubility Advantage

In order to approximate the solubility ratio of the amorphous to crystalline form, equation 1 was used (15):

$$\frac{\sigma^{amorph}}{\sigma^{crystal}} = e^{\frac{\Delta G}{RT}} \tag{1}$$

where $\sigma^{amorph}/\sigma^{crystal}$ represents the ratio of the solubility of the amorphous form to the solubility of the stable crystalline form. ΔG is the free energy difference between the amorphous and crystalline forms, R is the universal gas constant and T is the temperature in Kelvin. The free energy difference estimate is obtained from the Hoffman equation (24).

$$\Delta G = \frac{\Delta H_f \cdot \Delta T \cdot T}{T_m^2} \tag{2}$$

where ΔH_f is the enthalpy of fusion, T is the operating temperature, T_m is the melting temperature and ΔT is $T_m - T$. Enthalpies of fusion were measured using a TA Q2000 differential scanning calorimeter (TA Instruments, New Castle, DE), and analysis of the melting endotherms was performed using the TA Universal analysis software (TA Instruments, New Castle, DE). Solubility values of the α crystalline form of indomethacin were measured in the pH 2 dissolution media in the presence and absence of pre-dissolved polymer with the SI-Photonics UV spectrometer described above as well as a Cary 300 Bio UV spectrometer with WinUV software (Varian Inc., Palo Alto, CA). Presence of the polymers at the aforementioned concentration did not have an impact on the equilibrium solubility at either 25°C or 37°C. The equilibrium solubility values for felodipine were taken from Konno *et. al.* (25).

RESULTS

Felodipine

Fig. 2 shows the dissolution profiles for amorphous felodipine at 25°C and 37°C. The dissolution profile of crystalline felodipine at 37°C is included in the plot for reference. It should be noted that the dissolution experiments were performed under non-sink conditions in order to

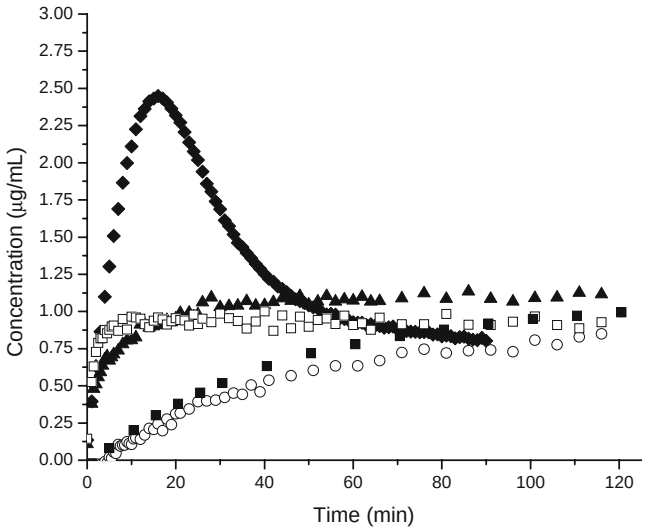

Fig. 2. Dissolution profiles of amorphous felodipine, where the amount of solid added per mL of dissolution medium was varied. At 25°C; 500 μg/mL (♦), 37°C; 100 μg/mL (○), 500 μg/ml (▲), 1,000 μg/mL (□) and crystalline felodipine (■).

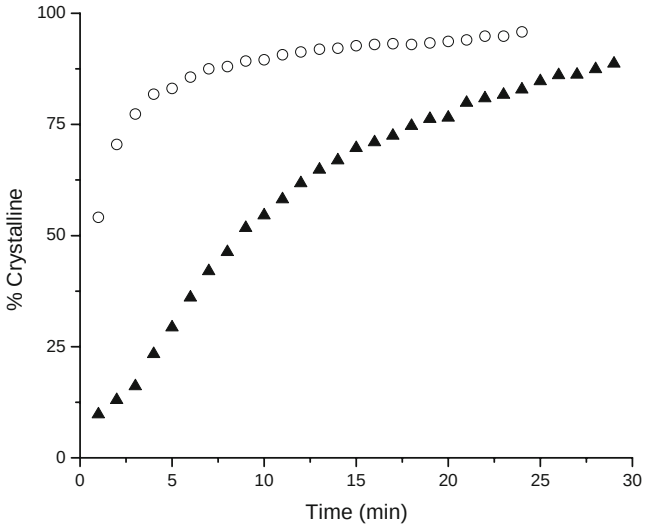

Fig. 3. Transformation kinetics of amorphous felodipine at 25°C (▲) and 37°C (○) determined using Raman spectroscopy.

evaluate the maximum solution concentration generated from an amorphous solid. Thus, the amount of solid added was in excess of the amount required to reach the equilibrium solubility of felodipine. For the dissolution of amorphous felodipine at 37°C, different amounts of solid were evaluated: 100 μg solid, 500 μg solid and 1,000 μg solid per mL of solution. It is apparent that the dissolution profile of 100 μg/mL (solid) of amorphous felodipine at 37°C is virtually identical to that of an equivalent mass of the crystalline material, reaching a plateau solution concentration of 1 μg/mL, which corresponds to the solubility of crystalline felodipine at 37°C (25). When the amount of amorphous solid is increased by a factor of 5 or 10, the maximum solution concentration generated is still approximately 1 μg/mL, although the dissolution rate is faster; hence, the maximum solution concentration is reached sooner. Thus, at 37°C, no "amorphous advantage" is observed for the felodipine system under these conditions. In contrast, at 25°C, the solution concentration reaches a maximum of about 2.50 μg/mL and then rapidly decreases. Thus, at 25°C a supersaturated solution is generated, which is followed by desupersaturation as a result of crystallization of felodipine from the solution phase. The final concentration measured is below 1 μg/mL.

In order to investigate the phase behavior, Raman spectroscopy was used to monitor the crystallinity of the solid material in contact with the dissolution medium as a function of time. Fig. 3 shows the resultant percent crystallinity *vs.* time plots which illustrate the transformation kinetics of felodipine slurried with the dissolution medium at both 37°C and 25°C. Amorphous felodipine commences crystallization immediately upon exposure to the dissolution medium at 37°C. After 1 min (first data acquisition point), the felodipine slurry is more than 50% crystalline. The extent of crystallinity then increases rapidly until the transformation is complete. These results explain why the dissolution profile of amorphous felodipine at 37°C looks very similar to that of the crystalline material. Essentially, the amorphous solid crystallizes more rapidly than it can dissolve on contact with the dissolution medium; hence, no supersaturation is generated. In contrast, Raman spectra from slurries at 25°C indicate that the crystallization kinetics are much slower than at 37°C, and approximately 8 min are required to reach 50% crystallinity. This delay in crystallization at 25°C enables some of the amorphous material to dissolve before it undergoes the solid state transformation resulting in a small extent of supersaturation, which reaches a peak at about 16 min as shown in Fig. 2.

Having established that no solubility advantage was provided by dissolution of amorphous felodipine at 37°C, it was of interest to investigate the impact of polymers dissolved in the dissolution medium on the concentration-time profile. Interestingly, when PVP, HPMC or HPMC-AS were predissolved in the medium at a concentration of 500 μg/mL, supersaturated solutions were generated upon dissolution of amorphous felodipine (500 μg solid per mL of dissolution media). The dissolution profiles of amorphous felodipine at

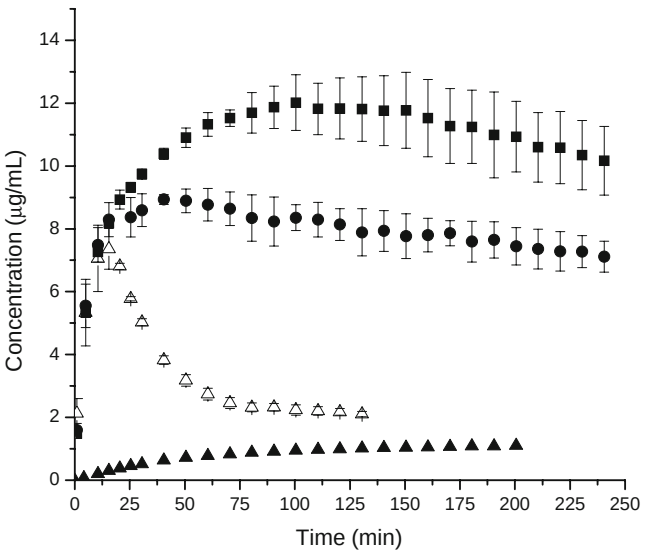

Fig. 4. Dissolution of profiles of amorphous felodipine at 37°C in the presence of various polymers pre-dissolved at a concentration of 500 μg/mL; PVP (Δ), HPMC (●) and HPMC-AS (■). Dissolution of crystalline felodipine at 37°C is included as a reference (▲).

37°C in the presence of polymers are shown in Fig. 4. The maximum supersaturation generated in the presence of each polymer is close to the theoretically calculated amorphous solubility advantage of around 9 μg/mL. This solubility advantage was calculated using equations 1 and 2 and the following values: enthalpy of fusion of 30.12 kJ/mol, melting temperature of 143.41°C and crystalline solubility of 1 μg/mL (37°C). In the case of PVP, the solution concentration reaches a peak of about 7.5 μg/mL, which then is followed by a rapid desupersaturation. In contrast, both HPMC and HPMC-AS were able to maintain the solution concentrations above 7 μg/mL and 10 μg/mL, respectively, for at least 4 h. For both of these polymers, there appears to be a slow decline in solution concentration once the maximum is reached. These results indicate that, in the case of felodipine, PVP is a poor inhibitor of crystallization from a supersaturated solution. In contrast, both HPMC and HPMC-AS are able to inhibit crystallization of felodipine from solution at the degree of supersaturation generated by the amorphous solid. These observations are in excellent agreement with previous results (25).

Fig. 5 shows the PXRD patterns of amorphous felodipine obtained 15 min after exposure to buffer in the presence and absence of HPMC-AS and PVP. The data clearly show that, in the absence of polymer, amorphous felodipine crystallizes within 15 min of exposure as indicated by the presence of the sharp diffraction peaks characteristic of crystalline felodipine. However, when PVP is present (1 mg/mL), there are no observable crystalline peaks after 15 min. At a concentration of 1 mg/mL, HPMC-AS also appears to be effective at delaying crystallization. After 15 min, the sample appears largely amorphous, although there is a small diffraction peak at 10° 2θ, indicating that crystallization is commencing.

The XRPD results suggest that the presence of PVP or HPMC-AS in the solution phase has a significant impact on the crystallization kinetics of the amorphous solid. Raman spectroscopy was used to further interrogate the crystallization kinetics in aqueous slurries containing the polymer. Percent crystallinity *vs.* time plots for felodipine slurried with a dissolution medium containing 500 μg/mL PVP, HPMC or HPMC-AS are shown in Fig. 6. The amorphous (37°C) data from Fig. 3 are included to provide a reference profile. For all of the polymers, a sigmoidal profile is obtained, indicating that there is a lag phase before crystallization begins, followed by a transformation period and then a plateau signaling the completion of the phase transformation. Thus, it appears that the polymers delay crystallization of the amorphous solid for a sufficient length of time such that a supersaturated solution can be generated through dissolution of the high energy amorphous form.

Indomethacin

Fig. 7 illustrates the concentration-time profiles of amorphous indomethacin dissolved at both 25°C and 37°C. As in the case of felodipine, the amount of solid added was in excess of the amount required to reach the equilibrium solubility of indomethacin. Only one amount of solid was used in all dissolution experiments: 300 μg solid per mL of solution. The peak solution concentration reached at 25°C is around 15 μg/mL, whereas at 37°C it is only 11.5 μg/mL. The theoretically calculated amorphous advantage at 25°C is 17–25 μg/ml, which is just above the maximum solution concentration levels generated upon dissolution at this temperature. The amorphous solubility estimates were based on equations 1 and 2 and an enthalpy of fusion of 32.48 kJ/mol, a melting temperature of 153.4°C and a crystalline solubility between 1 and 1.5 μg/mL (α form of indomethacin). At 37°C, the theoretically calculated solubility advantage is around 37 μg/ml based on the aforementioned enthalpy of fusion and melting temperature and a crystalline solubility of 3 μg/mL. It should be noted that the estimated solubility advantage at 37°C is substantially higher than that observed experimentally. At both temperatures, the solution concentrations drop once the maximum has been reached, suggesting that indomethacin is crystallizing from the supersaturated solution.

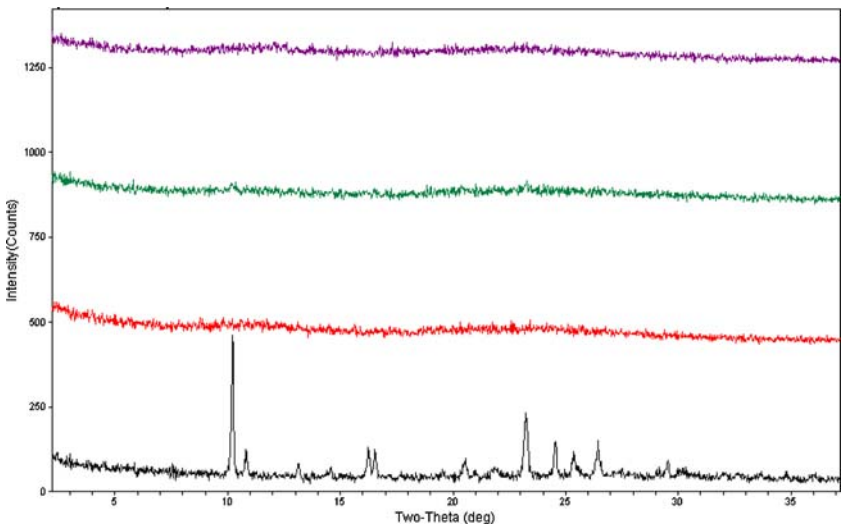

Fig. 5. PXRD patterns showing, from top to bottom, amorphous felodipine, amorphous felodipine exposed to dissolution media containing 1 mg/mL dissolved HPMC-AS, 1 mg/mL dissolved PVP and no polymer.

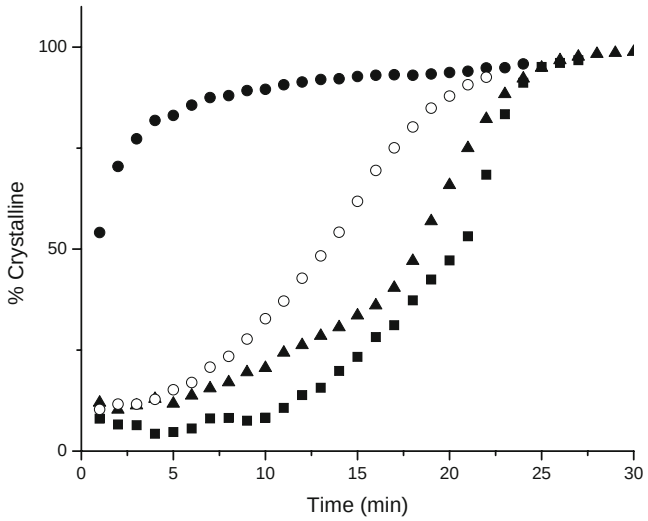

Fig. 6. Transformation kinetics of amorphous felodipine (37°C) with no polymer (●) and in the presence of various polymers dissolved at a concentration of 500 μg/mL; PVP (■), HPMC (▲), HPMC-AS (○).

The elevated solution concentration observed at 25°C (relative to 37°C) for indomethacin is similar to that seen for felodipine, albeit to a higher extent. In contrast to felodipine, supersaturation was also generated at 37°C. However, it should be noted that the results obtained at 37°C were complicated by a rapid agglomeration of the amorphous material to a few large particles. As a result, this led to an uncontrolled surface area with an unknown impact on the dissolution profile.

In order to better understand the dissolution of indomethacin, the phase behavior of the amorphous solid in contact with the aqueous medium was probed using Raman spectroscopy at both 25°C and 37°C. Fig. 8 illustrates representative Raman spectra of indomethacin after exposure to dissolution media at 25°C for 120, 180 and 240 min (alpha crystalline and amorphous spectra are provided for reference). As can be seen from both the carbonyl region between 1,600–1,800 cm^{-1}, which contains characteristic peaks of the

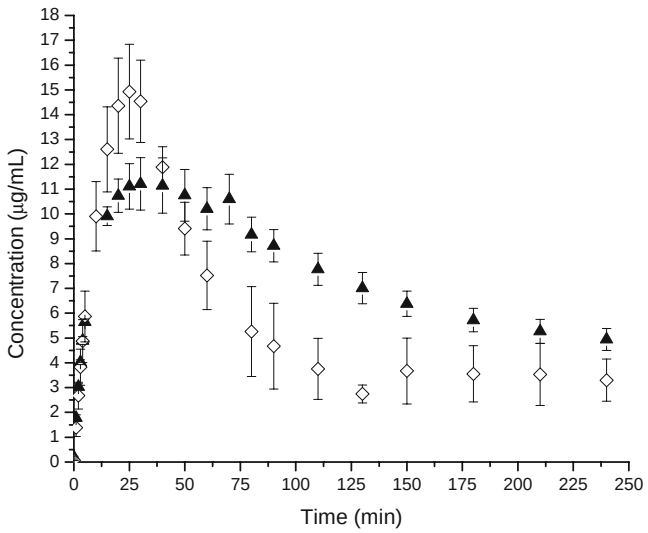

Fig. 7. Dissolution of amorphous indomethacin at 37°C (▲) and 25° (◊).

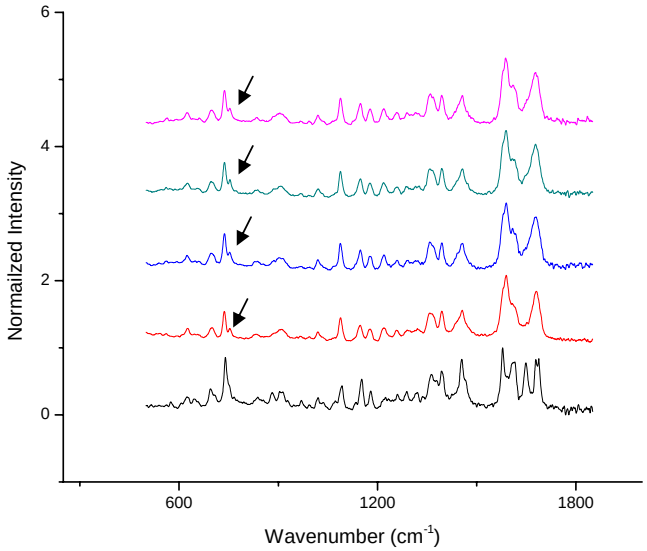

Fig. 8. Raman spectra of indomethacin slurries showing, from top to bottom, amorphous indomethacin 240 min, 180 min and 120 min after exposure to buffer (25°C), unexposed amorphous indomethacin and alpha indomethacin.

different forms, as well by monitoring a small peak at 753 cm^{-1} (indicated by the arrow) which is only present in the amorphous spectra, the slurried indomethacin remained amorphous for at least 4 h. This was confirmed with cross-polarized microscopy. In contrast, at 37°C, the sample was still largely amorphous after 20 min, but after 90 min, the presence of the alpha polymorph could clearly be observed, and after 120 min, the spectrum was similar to that of pure alpha (Fig. 9). These results clearly show that, at 37°C, amorphous indomethacin transformed to the crystalline alpha polymorph. The time course of the conversion at 37°C was estimated by monitoring the intensity of a peak unique to the alpha form of indomethacin and is shown in Fig. 10. This peak

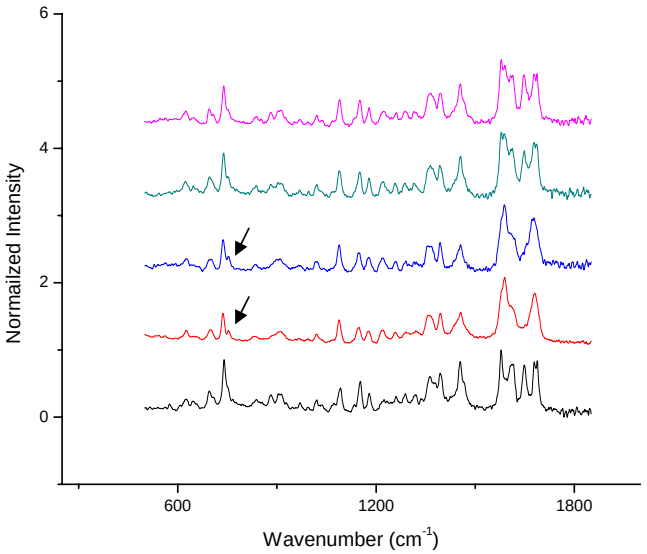

Fig. 9. Raman spectra of indomethacin slurries showing, from top to bottom, amorphous indomethacin 120 min, 90 min and 20 min after exposure to buffer (37°C), unexposed amorphous indomethacin and alpha indomethacin.

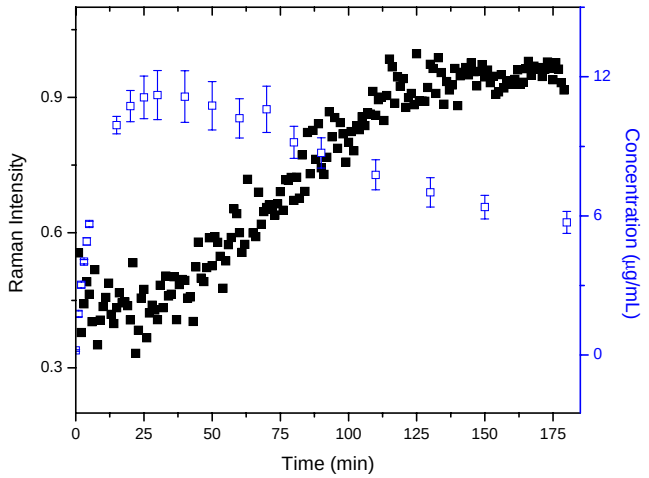

Fig. 10. Normailzed peak intensity (■) of alpha indomethacin at 1,648 cm^{-1} as a function of time and dissolution of amorphous indomethacin at 37°C as a function of time (□).

corresponds to the hydrogen bonded carbonyl of the amide group in indomethacin (26,27). This plot shows a lag phase of about 30 min, followed by a transformation phase that plateaus at around 120 min. When these solid state transformation kinetics are compared with the dissolution profile at 37°C, potential correlations between the two processes can be investigated. Figure 10 shows that the maximum in concentration in the dissolution profile occurs around the onset of the transformation of the amorphous solid to the crystalline phase. Crystallization of this solid would result in a reduction in the dissolution rate. In turn, the rate of dissolution relative to the rate of crystallization from solution would be altered. The combination of these events would ultimately add up to a reduction in the solution concentration as a function of time.

Dissolution of amorphous indomethacin in the presence of PVP (250 μg/mL pre-dissolved in the dissolution medium) yields an increase in the level of supersaturation (when compared with no polymer) at both 25°C and 37°C, as shown in Fig. 11. At 25°C, the maximum concentration reached is around 23.5 μg/mL. This value lies within the range estimated for the solubility of amorphous indomethacin (17–25 μg/mL). In addition, once generated, this solution concentration was maintained for the duration of the experiment (4 h). Thus, it appears that PVP is an effective inhibitor of solution crystallization at this temperature and supersaturation. At 37°C, the maximum solution concentration reached was the same as at 25°C. This maximum solution concentration was not maintained for the duration of the experiment and was less than the estimated amorphous solubility at this temperature (~37 μg/mL). A similar profile was achieved for the dissolution of amorphous indomethacin in the presence of HPMC (250 μg/mL) at 25°C as shown in Fig. 12. At 37°C, the observed dissolution behavior was different. The peak solution concentration achieved was much lower than in the presence of PVP. However, HPMC appeared to maintain the solution concentration more effectively at 37°C than PVP, albeit at a lower level of supersaturation. Several factors could lead to this observation, including a difference in the thermodynamic driving force for crystallization, a parameter which is directly linked with the degree of supersaturation.

The solid state phase transformation behavior of slurried amorphous indomethacin at 37°C was investigated in the presence of pre-dissolved PVP and HPMC (250 μg/mL) using Raman spectroscopy (data not shown). Although neither polymer appeared to result in a substantial delay in the onset of crystallization, a more rigorous study is needed in order to more accurately determine the onset of crystallization.

The effect of polymers on crystallization of indomethacin from solution was also evaluated, since unlike felodipine this information is not available in the literature. In order to assess the ability of the two polymers to inhibit solution crystallization, supersaturated solutions were generated in pH 2 dissolution media at both 25°C and 37°C, and solution concentration-time profiles were monitored. Results are shown in Figs. 13 and 14 for the experiments in the absence of polymer as well as in the presence of pre-dissolved PVP and HPMC (250 μg/mL). The artificially generated concentrations, around 40 μg/mL at 37°C and 25 μg/mL at 25°C, were chosen based on the theoretically calculated solubility

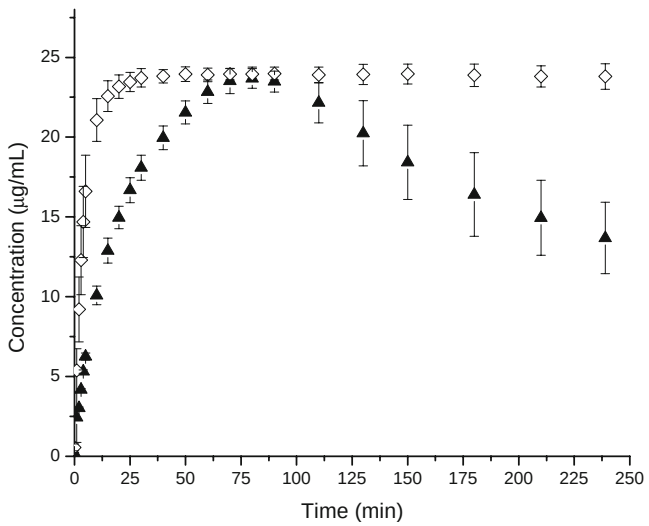

Fig. 11. Dissolution of amorphous indomethacin in the presence of 250 μg/mL dissolved PVP at 37°C (▲) and 25° (◊).

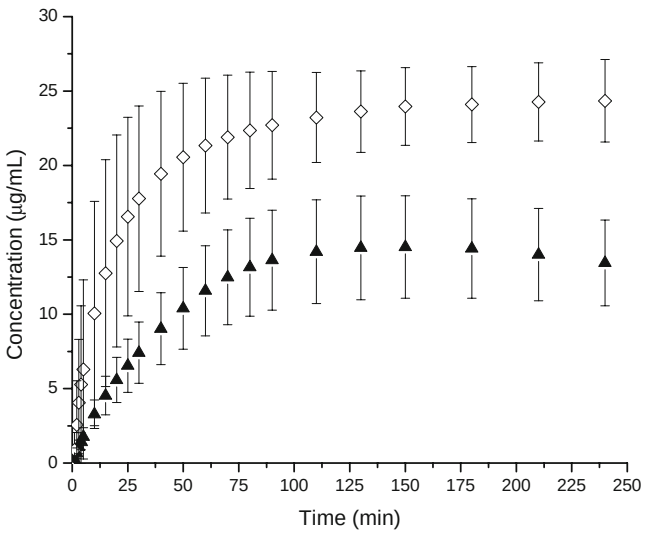

Fig. 12. Dissolution of amorphous indomethacin in the presence of 250 μg/mL dissolved HPMC at 37°C (▲) and 25° (◊).

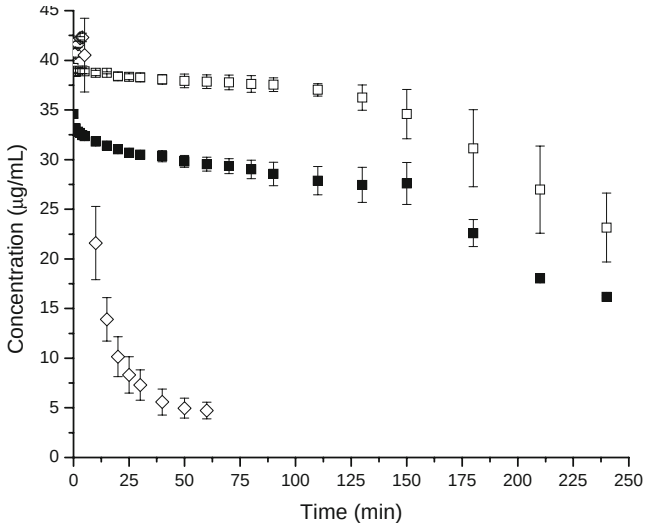

Fig. 13. Concentration-time profile of indomethacin in the absence of polymer (◊) and in presence of 500 μg/mL pre-dissolved PVP (■) and HPMC (□) at 37°C.

advantage provided by the amorphous form of indomethacin. It is clear from the data that both HPMC and PVP have the ability to inhibit crystallization of indomethacin from a supersaturated solution at both temperatures. At 37°C, in the absence of polymer, the solution concentration drops rapidly. The presence of HPMC results in maintenance of the initial solution concentration for about 2.5 h, and then the concentration starts to decrease. For the PVP-containing solutions, there is an initial drop in concentration to about 33 μg/mL, followed by a fairly steady concentration until 160 min, at which point the concentration begins to decrease. Based on these results, it would be expected that both polymers would be able to largely inhibit crystallization from solution at the supersaturations generated by dissolution of the amorphous solid (Fig. 7).

There is a slightly different behavior at 25°C. The initial concentration generated was around 25 μg/mL. There is a 25 min delay before desupersaturation takes place in the absence of polymer. In the presence of either polymer, there is a very slow desupersaturation that takes place throughout the 4 h experiment such that the final solution concentration is approximately 20 μg/mL. Thus, at 25°C, the polymers should be able to largely inhibit crystallization from solution at the supersaturation generated by dissolution of the amorphous material (Fig. 7).

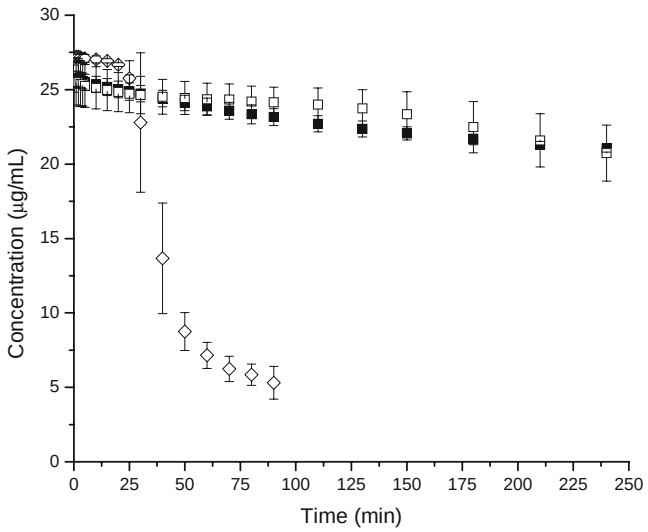

Fig. 14. Concentration time profile of indomethacin in the absence of polymer (◊) and in presence of 500 μg/mL pre-dissolved PVP (■) and HPMC (□) at 25°C.

Fig. 15 shows two micrographs obtained under cross polarized light of amorphous indomethacin exposed to pH 2 phosphate buffer (room temperature) initially (A) and after 1 h (B). In the absence of polymer, there are several areas, including the one highlighted, where dendritic needle-like crystals appear, indicating crystallization of indomethacin from the solution phase. It should also be noted that there is no evidence of crystallization of the amorphous indomethacin in solid state. Images were also taken with the solution containing both polymers (data not shown) at a solution concentration of 250 μg/mL. It was quite clear from the images that the formation of crystalline indomethacin (needle-like crystals) via a solution-mediated phase transformation was completely arrested.

DISCUSSION

Both the amorphous solid undergoing dissolution and the supersaturated solution generated from the dissolution of this solid are thermodynamically metastable or unstable and therefore may undergo a phase transformation to a lower free energy state. The kinetics of these phase changes relative to kinetics of dissolution will in large part shape the observed

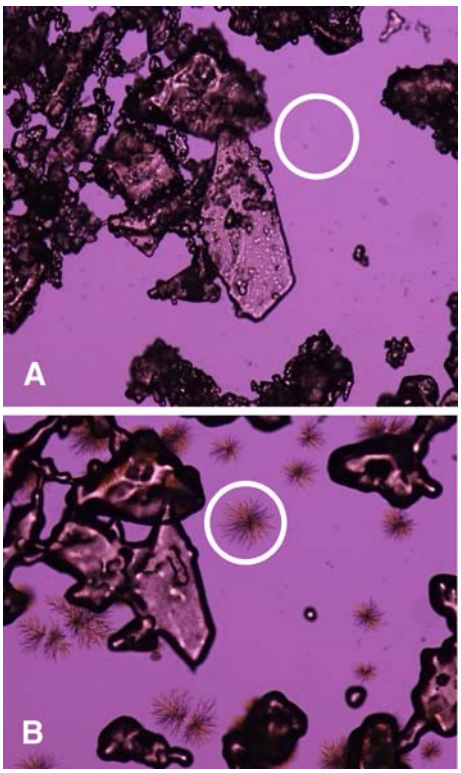

Fig. 15. Micrographs of amorphous indomethacin exposed to pH 2 buffer at room temperature initially (A) and after 60 min (B).

concentration-time profile. Hence, the concentration-time profiles generated during dissolution of amorphous materials are governed by several factors that need to be understood in order to effectively characterize the behavior of these systems. As was shown in the previous section, crystallization of the amorphous solid during dissolution can have a significant impact on the concentration-time profile. If the rate of crystallization of the amorphous material is sufficiently fast upon contact with the dissolution medium, it will not be possible to generate a solution concentration higher than that produced by the crystalline material. In other words, the material converts so fast that the observed profile looks similar to that of the crystalline material because it is the crystalline material that is dissolving. This is the case for amorphous felodipine at 37°C where no supersaturation is observed, and rapid crystallization of the amorphous solid on contact with the aqueous medium was confirmed using Raman spectroscopy. However, when the temperature was reduced to 25°C, supersaturation was observed. This difference can be explained by the difference in the crystallization rate of the solid at the two temperatures investigated; at 25°C, there was a clear reduction in crystallization rate of amorphous felodipine when compared to 37°C, based on the Raman spectroscopic evidence shown in Fig. 3. In considering the effect of temperature on the crystallization kinetics of the solid material, it is relevant to take into account that the glass transition temperature of dry felodipine is around 45°C and that of felodipine exposed to 75% RH is just below 35°C (28). Thus, the hydrated amorphous material at 37°C will be above Tg and therefore presumably subject to faster crystallization kinetics than the sample at 25°C.

Interestingly, addition of polymers to the dissolution medium delayed the crystallization of the solid amorphous phase. It was previously reported by Sato *et al.* that the presence of pre-dissolved HPMC inhibited the crystallization of amorphous 9,3-diacetylmidecamycin during dissolution (29). Our findings on amorphous felodipine are consistent with this previous observation. It would be reasonable to speculate that crystallization begins at the surface of the amorphous solid as observed for other amorphous solids (12,30,31) and that this surface crystallization would be exacerbated through plasticization by water. Given the low levels of polymer in solution, it would seem reasonable to speculate that the polymers act to inhibit crystallization of the solid material by interacting with the surface and delaying surface crystallization. Work by Yu *et al.* has demonstrated that a thin film of polymer on the surface of an amorphous particle can indeed inhibit surface crystallization (32). The inhibition of crystallization of amorphous felodipine subsequently resulted in solution concentrations peaking in the range 8–12 μg/mL; these solution levels are in reasonable agreement with the estimated value for the amorphous solubility of around 9 μg/mL. Therefore, through the inhibition of crystallization of the amorphous solid, it is possible to approach the "amorphous solubility advantage."

In addition to crystallization of the solid phase, crystallization kinetics from the solution phase also have to be considered when attempting to evaluate the advantage achieved through dissolution of amorphous materials. Once a supersaturated solution is generated and the solution concentration exceeds the metastable zone, nucleation followed by crystal growth can occur. This would lead to a depletion of the solution concentration towards the thermodynamic solubility. In order to have the desired impact on bioavailability, prevention of this desupersaturation is necessary. Previous studies have shown that crystallization of felodipine in the absence of polymer is rapid in aqueous solutions at a concentration of about 9 μg/mL. However, HPMC and HPMC-AS were able to substantially inhibit solution crystallization at this concentration, whereas PVP was much less effective (25). These previous observations are in agreement with the dissolution experiments presented in this article, where PVP is much less effective at maintaining superaturation than the cellulosic polymers. In contrast, its presence in solution is at least as effective as the other polymers at delaying crystallization of the solid material (Fig. 6). Based on the data shown here, the limiting factors that impact the dissolution of amorphous felodipine include crystallization from the solid as well as from solution. When both of these processes are substantially delayed, the solution concentration generated is close to the theoretically estimated values.

In the case of indomethacin, the solid amorphous material was much less susceptible to crystallization on contact with the dissolution medium. At 25°C, no crystallization of amorphous indomethacin was observed via Raman spectroscopy or cross-polarized microscopy, and as a result, significantly supersaturated solutions were generated upon dissolution. However, there was a solution-mediated crystallization that took place which subsequently reduced the solution concentration (Figs. 7 and 15). These observations indicate that the limiting factor in the dissolution of amorphous indomethacin at 25°C is crystallization from solution and that this is the process that needs to be inhibited in order to reach the estimated amorphous solubility. This was achieved successfully by adding small amounts of either PVP or HPMC to the solution. The situation is a little more complicated at 37°C because amorphous indomethacin agglomerates extensively, and this agglomeration would certainly be expected to delay dissolution. At this temperature, it is clear that the amorphous solid does crystallize over the timescale of the experiment (after about 90 min to the α form, Fig. 9). Although the polymers did inhibit crystalliza-

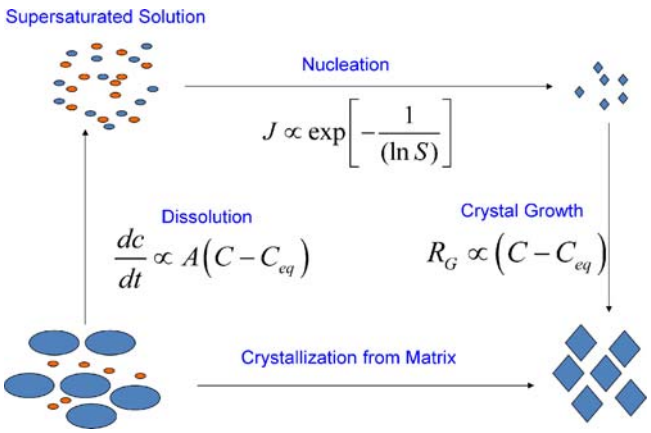

Fig. 16. Schematic illustrating the competition between dissolution and crystallization via the solid or solution state for amorphous systems.

tion from solution, they do not appear to be very effective at delaying the solid phase crystallization. Presumably, the lower extent of supersaturation reached at 37°C can be explained by a combination of delayed dissolution due to reduced surface area and subsequent crystallization of the solid material. It should be noted that the polymers appeared to be less effective at inhibiting solution crystallization at 37°C, which may also have an impact. Another interesting observation is that amorphous indomethacin either does not crystallize or does so much slower than amorphous felodipine at both temperatures. The glass transition temperature of indomethacin has been shown to rapidly decrease as a function of water content similar to felodipine (33). This, coupled with the fact that amorphous indomethacin has a larger driving force for crystallization than amorphous felodipine, would suggest that it should at least crystallize near the same rate as felodipine. However, the data presented show dramatic differences in the crystallization rates of these two compounds during dissolution. This is an indication of the complexity of the processes taking place in these systems and that a single parameter like the glass transition temperature will not fully explain the observed behavior (34).

Fig. 16 is a diagram that summarizes the important processes that can occur during dissolution of an amorphous system. In the dissolution path of this diagram, *dc/dt* represents the dissolution rate which is proportional to the surface area *A* and the difference between the solution concentration (*C*) and the equlibrium concentration (C_{eq}) as described by the modified Noyes and Whitney equation (35). In the nucleation path, *J* (36) represents the nucleation rate, which is proportional to the degree of supersaturation *S*. In the growth path, the rate of crystal growth is also proportional to the the difference between the actual solution concentration and the equlibrium concentration (37). If, as in the case of amorphous felodipine at 37°C, crystallization from the matrix is extremely rapid upon exposure to the dissolution media relative to the dissolution rate, no supersaturation will be observed. However, if crystallization from the matrix is slow relative to the dissolution rate, or does not take place, then any lack of performance of the amorphous material will be a result of crystallization from the supersaturated solution. The nucleation and growth proportionalities in Fig. 16 demonstrate the relationship that the higher the degree of supersaturation, the higher the nucleation and growth rates. Therefore, as the degree of supersaturation increases during dissolution of the amorphous material, the greater the likelihood of nucleation and growth from solution with a corresponding decrease in solution concentration. This was the case with indomethacin at 25°C and felodipine in the presence of pre-dissolved polymers where the solution-mediated transformation was the dominant mechanism for the depletion of elevated solution concentrations.

These observations are of great importance because it is likely that both routes of crystallization will be important for many compounds. Having a complete understanding of the relative contribution of each route will not only facilitate an understanding of the observed concentration-time profile generated on dissolution of the amorphous solid, but will also enable the stabilization potential of polymers, included as part of the formulation on each of these crystallization routes to be assessed. This type of assessment would be of relevance for the rational design of solid dispersions, where it would be resonable to speculate that certain amorphous APIs might be more effectively formulated using multiple polymers: one polymer optimal for stabilizing the amorphous solid with the other being the most effective solution crystallization inhibitor.

CONCLUSIONS

Amorphous solids can undergo crystallization during dissolution via two routes: crystallization of the solid material or crystallization from the supersaturated solution generated by dissolution of the amorphous solid. Amorphous felodipine was found to rapidly crystallize when introduced into dissolution media at 37°C, resulting in maximum solution concentrations equivalent to the equilibrium solubility of the crystalline form. At 25°C, crystallization of the solid material was reduced, and a small extent of supersaturation was achieved. Polymeric additives, present in the solution phase, were found to dramatically reduce the crystallization tendency of the amorphous solid during dissolution; consequently, supersaturated solutions were generated and were stabilized by the presence of the polymers. In the case of indomethacin, supersaturation was generated at both temperatures because the solid crystallized much slower on contact with the dissolution medium. Crystallization from solution was the predominant mechanism for reducing the solubility advantage for this compound. Again, polymeric additives were able to stabilize the supersaturated solutions to some extent. Understanding these phase changes will lead to an improved understanding of the potential solubility advantage of amorphous compounds and how this can be maximized through the addition of stabilizing additives.

ACKNOWLEDGMENTS

We would like to acknowledge the PhRMA foundation for providing a pre-doctoral fellowship to David Alonzo, as well as funding from Abbott Labs. A special thanks to Davor Gusak and Sajeda Abdo for their help in the laboratory.

REFERENCES

1. Leuner C, Dressman J. Improving drug solubility for oral delivery using solid dispersions. Eur J Pharm Biopharm. 2000;50:47–60.
2. Lipinski CA, Lombardo F, Dominy BW, Feeney PJ. Experimental and computational approaches to estimate solubility and permeability in drug discovery and development settings. Adv Drug Delivery Rev. 1997;23:3–25.
3. Ambike AA, Mahadik KR, Paradkar A. Spray-dried amorphous solid dispersions of simvastatin, a low Tg drug: *in vitro* and *in vivo* evaluations. Pharm Res. 2005;22:990–8.
4. Six K, Verreck G, Peeters J, Brewster M, Van den Mooter G. Increased physical stability and improved dissolution properties of itraconazole, a class II drug, by solid dispersions that combine fast- and slow-dissolving polymers. J Pharm Sci. 2004;93:124–31.
5. Yamashita K, Nakate T, Okimoto K, Ohike A, Tokunaga Y, Ibuki R, *et al.* Establishment of new preparation method for solid dispersion formulation of tacrolimus. Int J Pharm. 2003;267:79–91.
6. Kennedy M, Hu J, Gao P, Li L, Ali-Reynolds A, Chal B, *et al.* Enhanced bioavailability of a poorly soluble vr1 antagonist using an amorphous solid dispersion approach: a case study. Mol Pharm. 2008;5:981–93.

7. Kim MS, Jin SJ, Kim JS, Park HJ, Song HS, Neubert RHH, *et al*. Preparation, characterization and *in vivo* evaluation of amorphous atorvastatin calcium nanoparticles using supercritical antisolvent (SAS) process. Eur J Pharm Biopharm. 2008;69:454–65.
8. Law D, Schmitt EA, Marsh KC, Everitt EA, Wang WL, Fort JJ, *et al*. Ritonavir-PEG 8000 amorphous solid dispersions: *in vitro* and *in vivo* evaluations. J Pharm Sci. 2004;93:563–70.
9. Vaughn JM, McConville JT, Crisp MT, Johnston KP, Williams RO. Supersaturation produces high bioavailability of amorphous danazol particles formed by evaporative precipitation into aqueous solution and spray freezing into liquid technologies. Drug Dev Ind Pharm. 2006;32:559–67.
10. Marsac PJ, Konno H, Taylor LS. A comparison of the physical stability of amorphous felodipine and nifedipine systems. Pharm Res. 2006;23:2306–16.
11. Shamblin SL, Tang XL, Chang LQ, Hancock BC, Pikal MJ. Characterization of the time scales of molecular motion in pharmaceutically important glasses. J Phys Chem B. 1999;103:4113–21.
12. Wu T, Yu L. Surface crystallization of indomethacin below T-g. Pharm Res. 2006;23:2350–5.
13. Yu L. Amorphous pharmaceutical solids: preparation, characterization and stabilization. Adv Drug Delivery Rev. 2001;48:27–42.
14. Zhou D, Zhang GGZ, Law D, Grant DJW, Schmitt EA. Thermodynamics, molecular mobility and crystallization kinetics of amorphous griseofulvin. Mol Pharm. 2008;5:927–36.
15. Hancock BC, Parks M. What is the true solubility advantage for amorphous pharmaceuticals? Pharm Res. 2000;17:397–404.
16. Chikaraishi Y, Otsuka M, Matsuda Y. Dissolution phenomenon of the piretanide amorphous form involving phase change. Chem Pharm Bull. 1996;44:2111–5.
17. Fukuoka E, Makita M, Yamamura S. Glassy state of pharmaceuticals. 2. Bioinequivalence of glassy and crystalline indomethacin. Chem Pharm Bull. 1987;35:2943–8.
18. Savolainen M, Kogermann K, Heinz A, Aaltonen J, Peltonen L, Strachan C, *et al*. Better understanding of dissolution behaviour of amorphous drugs by *in situ* solid-state analysis using Raman spectroscopy. Eur J Pharm Biopharm. 2009;71:71–9.
19. Windbergs M, Jurna M, Offerhaus HL, Herek JL, Kleinebudde P, Strachan CJ. Chemical imaging of oral solid dosage forms and changes upon dissolution using coherent anti-stokes Raman scattering microscopy. Anal Chem. 2009;81:2085–91.
20. Konno H, Taylor LS. Influence of different polymers on the crystallization tendency of molecularly dispersed amorphous felodipine. J Pharm Sci. 2006;95:2692–705.
21. Matsumoto T, Zografi G. Physical properties of solid molecular dispersions of indomethacin with poly(vinylpyrrolidone) and poly(vinylpyrrolidone-co-vinylacetate) in relation to indomethacin crystallization. Pharm Res. 1999;16:1722–8.
22. Van den Mooter G, Wuyts M, Blaton N, Busson R, Grobet P, Augustijns P, *et al*. Physical stabilisation of amorphous ketoconazole in solid dispersions with polyvinylpyrrolidone K25. Eur J Pharm Sci. 2001;12:261–9.
23. Weuts I, Kempen D, Decorte A, Verreck G, Peeters J, Brewster M, *et al*. Physical stability of the amorphous state of loperamide and two fragment molecules in solid dispersions with the polymers PVP-K30 and PVP-VA64. Eur J Pharm Sci. 2005;25:313–20.
24. Hoffman JD. Thermodynamic driving force in nucleation and growth processes. J Chem Phys. 1958;29:1192–3.
25. Konno H, Handa T, Alonzo DE, Taylor LS. Effect of polymer type on the dissolution profile of amorphous solid dispersions containing felodipine. Eur J Pharm Biopharm. 2008;70:493–9.
26. Taylor LS, Zografi G. Spectroscopic characterization of interactions between PVP and indomethacin in amorphous molecular dispersions. Pharm Res. 1997;14:1691–8.
27. Towler CS, Taylor LS. Spectroscopic characterization of intermolecular interactions in solution and their influence on crystallization outcome. Cryst Growth Des. 2007;7:633–8.
28. Marsac PJ, Konno H, Rumondor ACF, Taylor LS. Recrystallization of nifedipine and felodipine from amorphous molecular level solid dispersions containing poly(vinylpyrrolidone) and sorbed water. Pharm Res. 2008;25:647–56.
29. Sato T, Okada A, Sekiguchi K, Tsuda Y. Difference in physicopharmaceutical properties between crystalline and noncrystalline 9, 3″-diacetylmidecamycin. Chem Pharm Bull. 1981;29:2675–82.
30. Zhu L, Wong L, Yu L. Surface-enhanced crystallization of amorphous nifedipine. Mol Pharm. 2008;5:921–6.
31. Ishida H, Wu TA, Yu LA. Sudden rise of crystal growth rate of nifedipine near T-g without and with polyvinylpyrrolidone. J Pharm Sci. 2007;96:1131–8.
32. Wu T, Sun Y, Li N, de Villiers MM, Yu L. Inhibiting surface crystallization of amorphous indomethacin by nanocoating. Langmuir. 2007;23:5148–53.
33. Andronis V, Yoshioka M, Zografi G. Effects of sorbed water on the crystallization of indomethacin from the amorphous state. J Pharm Sci. 1997;86:346–51.
34. Bhugra C, Pikal MJ. Role of thermodynamic, molecular, and kinetic factors in crystallization from the amorphous state. J Pharm Sci. 2008;97:1329–49.
35. Lachman L, Lieberman HA, Kanig JL. The theory and practice of industrial pharmacy. Stipes Publishing LLC, 1986.
36. Mullin JW. Crystallization. 4th ed. Oxford: Elsevier Butterworth-Heinemann; 2001.
37. Garside J, Mersmann A, Nyvlt J. Measurement of Crystal Growth and Nucleation Rates. 2nd ed. Rugby: Institute of Chemical Engineers; 2002.